Eur. Phys. J. C 43, 51–57 (2005)
Digital Object Identifier (DOI) 10.1140/epjc/s2005-02261-6

THE EUROPEAN PHYSICAL JOURNAL C

Heavy quark potentials and quarkonium binding

P. Petreczky[a]

Nuclear Theory Group, Department of Physics, Brookhaven National Laboratory, Upton, New York 11973-500, USA

Received: 16 February 2005 /
Published online: 31 May 2005 –

Abstract. I review recent progress in studying in-medium modification of inter-quark forces at finite temperature in lattice QCD. Some applications to the problem of quarkonium binding in potential models are also discussed.

PACS. 11.15.Ha, 11.10.Wx, 12.38.Mh, 25.75.Nq

1 Introduction

The study of in-medium modifications of inter-quark forces at high temperatures is important for a detailed theoretical understanding of the properties of the quark–gluon plasma as well as for the detection of its formation in heavy ion collisions. In particular, it was suggested by Matsui and Satz that color screening at high temperature will result in dissolution of the quarkonium state, and the corresponding quarkonium suppression could be a signal of quark–gluon plasma formation [1].

Usually the problem of in-medium modification of inter-quark forces is studied in terms of so-called finite temperature heavy quark potentials, which are, in fact, the differences in the free energies of the system with a static quark–antiquark pair and the same system without static charges. Alternatively this problem can be studied in terms of finite temperature quarkonium spectral functions [2–4]; for further recent work, see [5–7]. Recently substantial progress has been made in studying the free energy of static quark–antiquark pair which I am going to review in the present paper. An important question is what can we learn about the quarkonium properties from the free energy of static charges; this will be discussed at the end of the paper.

2 The free energy of static charges

Following McLerran and Svetitsky [8] the partition function of the system with static quark–antiquark ($Q\bar{Q}$) pair at finite temperature T can be written as

$$Z_{Q\bar{Q}}(r,T) = \langle W(\boldsymbol{r})W^\dagger(0)\rangle Z(T), \tag{1}$$

where $Z(T)$ is the partition function of the system without static charges and

$$W(\boldsymbol{x}) = \mathcal{P}\exp\left(\mathrm{i}g\int_0^{1/T}\mathrm{d}\tau A_0(\tau,\boldsymbol{x})\right) \tag{2}$$

is the temporal Wilson line. $L(\boldsymbol{x}) = \mathrm{Tr}W(\boldsymbol{x})$ is also known as a Polyakov loop and in the case of pure gauge theory it is an order parameter of the deconfinement transition. As the $Q\bar{Q}$ pair can be either in a color singlet or octet state, one should separate these irreducible contributions to the partition function. This can be done using the projection operators P_1 and P_8 onto color singlet and octet states introduced in [9,10]. Applying P_1 and P_8 to $Z_{Q\bar{Q}}(r,T)$ we get the following expression for the singlet and octet free energies of the static $Q\bar{Q}$ pair:

$$\begin{aligned}\exp(-F_1(r,T)/T) &= \frac{1}{Z(T)}\frac{\mathrm{Tr}P_1 Z_{Q\bar{Q}}(r,T)}{\mathrm{Tr}P_1}\\ &= \frac{1}{3}\mathrm{Tr}\langle W(\boldsymbol{r})W^\dagger(0)\rangle \qquad (3)\\ \exp(-F_8(r,T)/T) &= \frac{1}{Z(T)}\frac{\mathrm{Tr}P_8 Z_{Q\bar{Q}}(r,T)}{\mathrm{Tr}P_8}\\ &= \frac{1}{8}\langle \mathrm{Tr}W(\boldsymbol{r})\mathrm{Tr}W^\dagger(0)\rangle - \frac{1}{24}\mathrm{Tr}\langle W(\boldsymbol{r})W^\dagger(0)\rangle. \qquad (4)\end{aligned}$$

Although usually $F_{1,8}$ is referred to as the free energy of the static $Q\bar{Q}$ pair, it is important to keep in mind that it refers to the difference between the free energy of the system with static quark–antiquark pair and the free energy of the system without static charges.

As $W(\boldsymbol{x})$ is a not gauge invariant operator, we have to fix a gauge in order to define F_1 and F_8. As we want that F_1 and F_8 have a meaningful zero temperature limit we better to fix the Coulomb gauge because in this gauge a transfer matrix can be defined and the free energy difference can be related to the interaction energy of a static $Q\bar{Q}$ pair at zero temperature ($T = 0$). Another possibility

[a] e-mail: petreczk@bnl.gov

discussed in [11] is to replace the Wilson line by a gauge invariant Wilson line using the eigenvector of the spatial covariant Laplacian [11]. For the singlet free energy both methods were tested and they were shown to give numerically indistinguishable results, which in the zero temperature limit are the same as the canonical results obtained from Wilson loops. The interpretation of the color octet free energy at small temperatures is less obvious and will be discussed separately. One can also define the color averaged free energy

$$\exp(-F_{\rm av}(r,T)/T) = \frac{1}{Z(T)}\frac{{\rm Tr}(P_1+P_8)Z_{Q\bar{Q}}(r,T)}{{\rm Tr}(P_1+P_8)} = \frac{1}{9}\langle {\rm Tr}W(\boldsymbol{r}){\rm Tr}W^\dagger(0)\rangle, \quad (5)$$

which is expressed entirely in terms of gauge invariant Polyakov loops. This is the reason why it was extensively studied on lattice during the last two decades. The color averaged free energy is a thermal average over the free energies in color singlet and color octet states,

$$\exp(-F_{\rm av}(r,T)/T) = \frac{1}{9}\exp(-F_1(r,T)/T) + \frac{8}{9}\exp(-F_8(r,T)/T). \quad (6)$$

Therefore it gives less direct information about medium modification of inter-quark forces. Given the partition function $Z_{Q\bar{Q}}(r,T)$ we can calculate not only the free energy but also the entropy as well as the internal energy of the static charges

$$S_i(r,T) = \frac{\partial}{\partial T}\ln\left(T\frac{Z^i_{Q\bar{Q}}(r,T)}{Z(T)}\right) = -\frac{\partial F_i(r,T)}{\partial T}, \quad (7)$$

$$U_i(r,T) = T^2\frac{\partial}{\partial T}\ln\left(\frac{Z^i_{Q\bar{Q}}(r,T)}{Z(T)}\right) = F_i(r,T) + TS_i(r,T), \quad i = 1, 8, {\rm av}. \quad (8)$$

3 Free energy of a static $Q\bar{Q}$ pair and screening of inter-quark forces at high temperatures

Perturbatively the quark–antiquark potential can be related to the scattering amplitude corresponding to one gluon exchange, and in the non-relativistic limit it is given by

$$V(r) = \langle T^aT^b\rangle g^2\int\frac{{\rm d}^3k}{(2\pi)^3}{\rm e}^{{\rm i}\boldsymbol{k}\cdot\boldsymbol{r}}D_{00}(k). \quad (9)$$

Here $D_{00}(k)$ is the temporal part of the Coulomb gauge gluon propagator, and in general it has the form

$$D_{00}(k) = (\mathbf{k}^2 + \Pi_{00}(\mathbf{k}))^{-1}.$$

Furthermore the averaging over color gives $\langle T^aT^b\rangle = -4/3$ for the color singlet and $\langle T^aT^b\rangle = +1/6$ for the color octet case. At zero temperature the polarization operator Π_{00} gives rise only to running of the coupling constant $g = g(r)$ (recall that $\alpha_{\rm s} = g^2/(4\pi)$). But at finite temperature T it has a non-trivial infrared limit, $\Pi_{00}(k\to 0) = m_D^2 = gT\sqrt{N_c/3 + N_f/6}$. Therefore at distances $r \gg 1/T$ the potential has the form

$$V(r,T) = \langle T^aT^b\rangle\frac{g^2}{4\pi r}\exp(-m_Dr). \quad (10)$$

The singlet and octet free energies defined in the previous section can also be easily calculated in leading order perturbation theory. Again because of $\Pi_{00}(k=0) = m_D^2$ one has

$$F_{1,8}(r,T) = \left(-\frac{4}{3},\frac{1}{6}\right)\frac{g^2}{4\pi r}\exp(-m_Dr). \quad (11)$$

In leading order the singlet free energy has exactly the same form as the potential and has no entropy contribution. This is the reason why the free energies of a static $Q\bar{Q}$ pair were (mis)interpreted as potentials. In next to leading order, which is $\mathcal{O}(g^3)$, the free energies have the form

$$F_{1,8}(r,T) = \left(-\frac{4}{3},\frac{1}{6}\right)\frac{g^2}{4\pi r}\exp(-m_Dr) - \frac{g^2m_D}{3\pi}, \quad (12)$$

and the entropy contribution $-TS$ appears (recall (7)). For the singlet case the entropy has the form

$$S_1(r,T) = \frac{g^2m_D}{3\pi T}(1-\exp(-m_Dr)). \quad (13)$$

It has the asymptotic value of $g^2m_D/3\pi T$ at large distances and vanishes for $rT \ll 1$. Similarly one can calculate the color octet entropy to be

$$S_8(r,T) = \frac{g^2m_D}{3\pi T}\left(1+\frac{1}{8}\exp(-m_Dr)\right). \quad (14)$$

Contrary to the color singlet case it does not vanish at small distances. We can also calculate the internal energy, which for the color singlet state, for example, can be written as

$$U_1(r,T) = -\frac{4}{3}\frac{g^2}{4\pi r}\exp(-m_Dr) - \frac{g^2m_D}{3\pi}\exp(-m_Dr), \quad (15)$$

and unlike the free energy vanishes at large distances (at least to order g^3). Using (6) and (11) one can easily get the perturbative result for the color averaged free energy. For $rT > 1$ the exponentials in (6) can be expanded and we arrive at the well known leading order result [8,10]

$$F_{\rm av}(r,T) = -\frac{1}{9}\frac{g^4}{(4\pi r)^2T}\exp(-2m_Dr). \quad (16)$$

4 Numerical results for the free energy of static $Q\bar{Q}$

4.1 Color singlet free energy

In this section I am going to review recent lattice results on the free energy of a static quark–antiquark pair. I will start

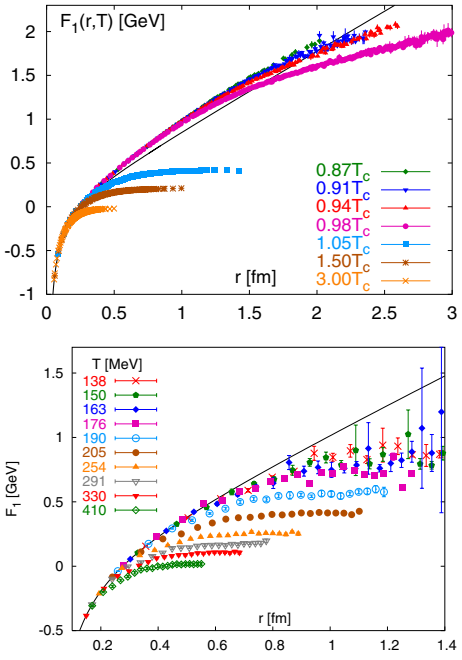

Fig. 1. The color singlet free energy in quenched [12,25] (top) and three flavor [16] (bottom) QCD. The solid black line is the $T = 0$ singlet potential

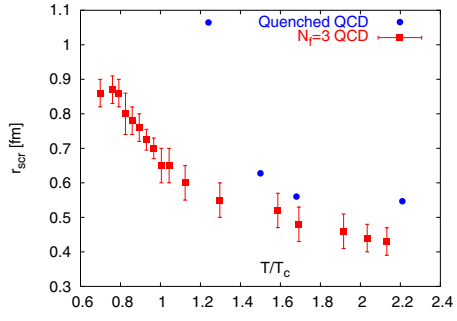

Fig. 2. The effective screening radius versus T/T_c [16]

the discussion with the case of the color singlet channel. The color singlet free energy has been extensively studied only during the last three years. Presently, results are available for SU(2) and SU(3) gauge theories [11–15] as well as in two flavor [17] and three flavor QCD [16]. While for pure gauge theories these studies are very systematic and lattice artifacts are under control, for full QCD they are still in the exploratory stage.

In Fig. 1 the singlet free energy for SU(3) gauge theory (QCD without dynamical quarks or quenched QCD) is shown for different temperatures together with the zero temperature quark–antiquark potential. For temperatures below the transition temperature $T_c \simeq 270\,\mathrm{MeV}$ the free energy rises linearly with the distance r signaling confinement. Above deconfinement, $T > T_c$, the free energy has a finite value at infinite separation indicating screening. One can also see from the figure that at short distances, $rT \ll 1$, the free energy is temperature independent in the entire temperature range and equal to the zero temperature potential. The singlet free energy for three flavor QCD is also shown in Fig. 1. The main difference compared to the case of SU(3) gauge theory is the fact that the free energy reaches a constant value at all temperatures. At low temperatures this is interpreted as string breaking; the flux tube breaks if enough energy is accumulated to create a light quark–antiquark pair, with which the static $Q\bar{Q}$ could form static-light mesons, i.e. when $V(r = r_{\mathrm{scr}}) = E^{\mathrm{binding}}_{\mathrm{heavy-light}}$ (see e.g., the discussion in [18]). The distance r_{scr}, at which the free energy effectively flattens off, depends on the temperature; it becomes smaller as the temperature increases. Therefore it is interpreted as an effective screening radius and is shown in Fig. 2. At low temperatures, $T < T_c$, it has a value of about 0.9 fm and rapidly decreases near the transition point. While close to T_c the effect of dynamical quarks is important for the value of the screening radius, at high temperatures the value of the screening radius is similar in quenched and full QCD.

4.2 Color octet free energy

The color octet free energy is shown in Fig. 3 for quenched QCD. At short distances it is repulsive, as expected from perturbation theory. Above the deconfinement temperature it has a strong temperature dependence which presumably comes from the entropy contribution and is present even at short distances. At high temperatures this is also expected from perturbation theory (see previous section). Above deconfinement the color octet free energy has the same large distance asymptotic value as the color singlet free energy $F_8(r \to \infty, T) = F_1(r \to \infty, T) = F_\infty(T)$. This is intuitively expected; at large distances the quark and antiquark are screened by their respective "clouds" and do not know anything about their relative color orientation. One should note that also below T_c the octet and singlet free energies become equal at large distances (compare Figs. 1 and 3), although there is no particular physical reason for this. I will discuss this problem at the end of this subsection. These features of the color octet free energy are present also in the case of three flavor QCD [16].

Perturbation theory predicts that at high temperatures we expect for the ratio $\delta F_1(r,T)/\delta F_8(r,T) \simeq -8$, where $\delta F_{1,8}(r,T) = (F_{1,8}(r,T) - F_\infty(T))$. In Fig. 4, the

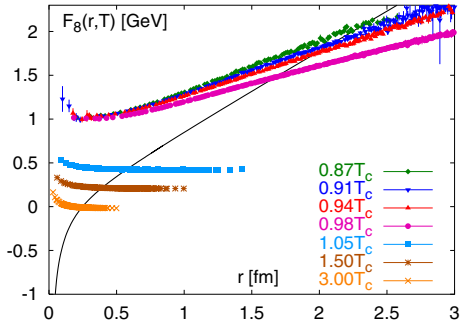

Fig. 3. The color octet free energy in quenched QCD [25]. The solid black line is the zero temperature singlet potential

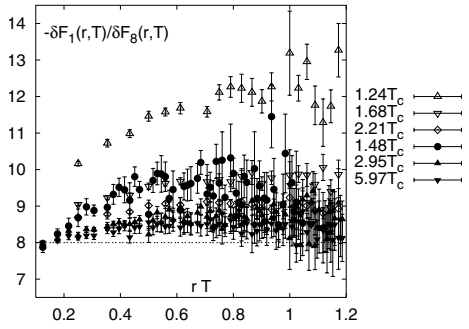

Fig. 4. The ratio of color singlet and color octet free energies [25]

lattice data in SU(3) gauge theory are confronted with these expectations. As one can see, the data are close to -8 for temperatures $T > 2T_c$.

While at high temperatures the meaning of the notion of color octet free energy is clear, the meaning of this quantity at low temperatures ("confinement region") is less evident. To understand the problem, let us first discuss the spectrum of static quark–antiquark free energies at zero temperature. The lowest energy level of a static $Q\bar{Q}$ pair is the one where the quark and antiquark are in a color singlet state. The corresponding energy as a function of the quark–antiquark separation is the singlet static potential, or simply the static potential, determined in terms of Wilson loop and used extensively in potential models (see [19,20]). There are also higher energy levels, whose energy functions are called hybrid potentials, for which the gluon fields between the static charges are in an excited state (or in other words, the string formed between the quark and antiquark is excited) [19,21,22]. The spectrum of hybrid potentials is shown in Fig. 5. The hybrid potentials are labeled by the angular momentum projection of the gluon field configurations on the quark–antiquark axis, $L = 0, 1, 2$ (denoted as Σ, Π, Δ), CP (even: g, or odd: u), and the reflections properties with respect to the plane passing through the quark–antiquark axis (even: $+$, or odd: $-$) [19]. The most distinct feature of the hybrid

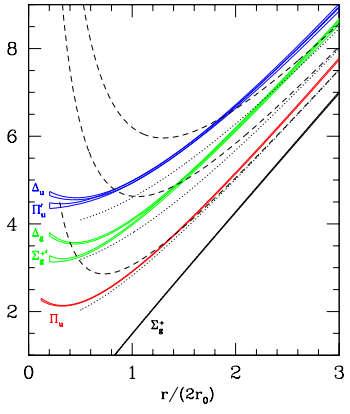

Fig. 5. The hybrid potentials in quenched QCD [21]. $\Sigma_g^+(r) = V(r)$ is the singlet potential and the dashed lines are predictions from the string model

potentials is the different slope at small distances, i.e., in contrast to the singlet potential the hybrid potentials are repulsive. They have a shape which is similar to the shape of the octet free energy at low temperatures, shown in Fig. 3. It has been shown that at short distances hybrid potentials correspond to the perturbative color octet potential [23]. This means that at short distances hybrid potentials correspond to a state in which the static $Q\bar{Q}$ pair is in an octet state and the net color charge is compensated by a soft gluon field which makes the whole object a color singlet (obviously only singlet objects can exist in the confinement region). At very small distances the soft gluon field is decoupled and the energy is dominantly determined by the large repulsive interaction of the static quark and antiquark [23].

The correlators which enter the definition of the color singlet and octet free energy have the following spectral representation [24]:

$$\langle \mathrm{Tr} W(\boldsymbol{r}) \mathrm{Tr} W^\dagger(0)\rangle = \sum_n \mathrm{e}^{-E_n(r,T)/T}, \qquad (17)$$

$$\langle \mathrm{Tr} W(\boldsymbol{r}) W^\dagger(0)\rangle = \sum_n c_n \mathrm{e}^{-E_n(r,T)/T}, \qquad (18)$$

where E_n denotes the different energy levels of the quark–antiquark system: singlet potential, hybrid potentials, singlet potentials plus glueballs, etc. The weights c_n in general are different from one and may have a non-trivial r-dependence [24]. Because of asymptotic freedom, c_1 should approach unity at short distances, while $c_{n>1}$ should vanish; at short distances, perturbation theory can be applied and the correlator $\langle \mathrm{Tr} W(\boldsymbol{r}) W^\dagger(0)\rangle$ gives the singlet potential. The tendency of c_1 approaching unity is clearly seen in the lattice data presented in [24]. Since the gap between the zero temperature (ground state) potential and the lowest hybrid potential is large for not too large distances, the color octet free energy is expected to be given by

$$\mathrm{e}^{-F_8(r,T)/T} \simeq \frac{1 - c_1(r)}{N^2 - 1} \mathrm{e}^{-E_1(r)/T}, \quad E_1(r) = V(r), \qquad (19)$$

i.e. it is determined by the singlet potential $V(r)$. This is the reason why at very large distances the color singlet and color octet free energies are equal in the low temperature region (compare Figs. 1 and 3). On the other hand, for sufficiently small distances $1 - c_1(r) \simeq 0$, and the octet free energy is expected to be determined by the lowest lying hybrid potential $F_8(r,T) \simeq E_2(r) + T \ln 8$.

4.3 Running coupling constant at finite temperature

To study how the free energies approach the zero temperature limit as well as to make contact with perturbation theory at short distances, it is convenient to introduce the effective running coupling constant $\alpha_{\mathrm{eff}}(r)$. This quantity can be also used to quantify the strength of the interaction, at least within the perturbative framework. At zero temperature the most convenient way to introduce the

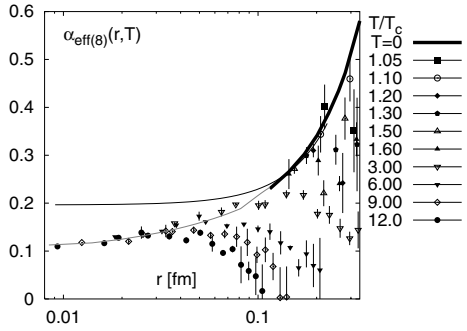

Fig. 6. The quenched running coupling constant at finite temperature in the color octet case [25]. The thick black line represents the lattice data at zero temperature. The thin black line is derived from a Coulomb plus linear parametrization of the zero temperature potential. The thin gray line is the 3-loop running coupling in the qq scheme [26]

effective running coupling constant is through the force between quark and antiquark, $\alpha_{\rm eff}(r) = (3/4)\cdot r^2({\rm d}V/{\rm d}r)$. This definition avoids many problems in the perturbative calculation of the effective coupling constant [26]. One can define similar quantities at finite temperatures [15,27]: $\alpha_{\rm eff\ 1,8}(r,T) = (3/4,-6)\cdot r^2({\rm d}F_{1,8}(r,T)/{\rm d}r)$ For the color singlet case in quenched QCD, $\alpha_{\rm eff}$ was discussed in detail in [15], where it was also pointed out that $\alpha_{\rm eff\,1} \simeq \alpha_{\rm eff\,8}$. In Fig. 6, the running coupling constant is shown for the octet case (the results in the singlet case are essentially identical). At short distances the effective coupling constant is temperature independent and coincides with the zero temperature result. At larger distances its deviates from the zero temperature result and after approaching a maximum, it drops because of the onset of screening. Note that for temperatures just above $T_{\rm c}$, the effective running coupling constant follows the zero temperature running coupling up to distances of about 0.3 fm. At such distances, the running coupling is not controlled by perturbation theory, but rather by the linear part of the potential, which gives a nearly quadratic rise for this quantity. Thus some non-perturbative confining physics survives deconfinement.

5 Entropy and internal energy of a static quark–antiquark pair

As was noted in Sect. 2, given the partition function $Z_{Q\bar{Q}}$, we can calculate the entropy and internal energy difference between the system with static charges and the same system without them; for the sake of simplicity, we call this difference the entropy and internal energy of $Q\bar{Q}$. Using (7) and (8), the entropy and internal energy has been calculated for infinite separation in quenched [14], two flavor [17] and three flavor [16] QCD. The results are shown in Fig. 7. Both the entropy and the internal energy show a very large increase near $T_{\rm c}$. For quenched QCD, the internal energy has been calculated for any separation r [14], and the results are shown in Fig. 8. One can see that with the exception of the small distance region, where the internal energy coincides with the zero temperature potential, the internal energy is larger than the free energy. In the high temperature limit, the internal energy has no constant part at large distances proportional to the temperature, so that it is tempting to interpret the free energies as potentials. However, the large increase of $U(r,T)$ near $T_{\rm c}$ makes such an interpretation problematic.

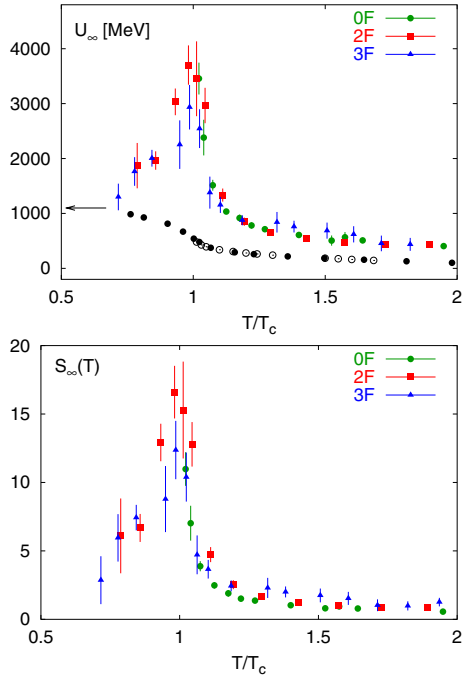

Fig. 7. The internal energy (top) and entropy (bottom) of a static $Q\bar{Q}$ pair at infinite separation in quenched [25], two flavor [17] and three flavor QCD [16]. The filled and open black circles give the free energy in two flavor and quenched QCD, respectively

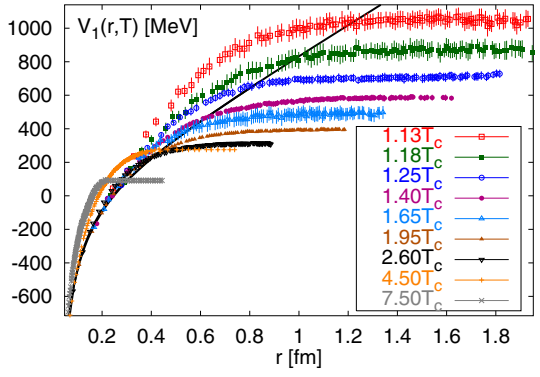

Fig. 8. The internal energy in quenched QCD [14]. The solid black line is the $T = 0$ potential

6 Quarkonium binding at finite temperature

Following the suggestion by Matsui and Satz [1], the problem of quarkonium binding at finite temperature has been studied using potential models with some phenomenological screened potential (see e.g. [28–30]). This led to

the conclusion that the J/ψ dissolves in the quark–gluon plasma at temperatures close to T_c. More recently, the free energy has been used as the potential in the Schrödinger equation, and it was found that the J/ψ can survive only up to temperature $1.1T_c$ [31]. As the free energy contains an r-dependent entropy contribution, the validity of this approach is doubtful. Finally, very recently the internal energy calculated in [14] was used as a potential in Schrödinger equation [32], and it was found that J/ψ can survive till $1.7T_c$ which is not inconsistent with lattice calculations of the J/ψ spectral function [3,4]. However, to test the validity of potential models, it is not sufficient to make statements about the dissociation temperature of a given quarkonium state; one should also investigate the change in the properties of heavy quarkonium bound states. For example, potential models with screening predict a decrease in the quarkonium masses. The most convenient way to compare the prediction of potential models with direct calculation of quarkonium spectral functions is to calculate the Euclidean meson correlator at finite temperature [34]. This quantity can be reliably calculated on the lattice. The basic idea is to use the model spectral function

$$\sigma(\omega,T) = \sum_i 2F_i(T)\delta(\omega^2 - M_i^2(T)) + m_0\theta(\omega - s_0(T))\omega^2,$$

containing bound states (resonances) and continuum [33, 34]. For a given screened potential one can solve the Schrödinger equation and determine the radial wave function (or its derivative) at the origin $R_i(0)$, and the binding energy E_i. The parameters of the model spectral functions can be related to these quantities, $F_i(T) \sim |R(0)|^2$, $M_i = 2m_{c,b} + E_i$, and acquire a temperature dependence because of the temperature dependence of the potential. Here $m_{c,b}$ are the constituent quark mass of c- and b-quarks. The threshold of the continuum $s_0(T)$ can be related to the asymptotic value of the potential at infinite distance, $s_0(T) = 2m_{c,b} + V_\infty(T)$. Having specified completely the spectral function of the model, the Euclidean correlator can be calculated

$$G(\tau,T) = \int_0^\infty \mathrm{d}\omega\sigma(\omega,T)\frac{\cosh(\omega(\tau - 1/(2T)))}{\sinh(\omega/(2T))} \qquad (20)$$

and compared with lattice results [34]. The Euclidean correlator can be reliably calculated on lattice, while extracting the spectral function from it is quite difficult. Using this approach some of the features of the quarkonium correlators, such as the enhancement of the scalar correlator above deconfinement temperature observed in lattice calculation, can be understood. A more detailed discussion on this topic is given in [34].

7 Conclusions

Free energies of static $Q\bar{Q}$ pairs have been extensively studied on the lattice and provide a useful tool to study the in-medium modification of inter-quark forces. Many-body effects exert a large influence on the free energy, thus making the simple picture in which the temperature dependence of the free energy reflects the screening of the two-body potential not applicable. Many-body effects are most prominent close to the transition temperature. For temperatures not too close to the transition temperature, the free energies of static quark–antiquark pairs could provide useful qualitative (though not quantitative) insights into the problem of quarkonium binding in a quark–gluon plasma. It is interesting to note in this respect that a new model approach to the problem of heavy quark potentials at finite temperature was recently proposed in [35].

Acknowledgements. This work was partly supported by U.S. Department of Energy under contract DE-AC02-98CH10886. P.P. is Goldhaber and RIKEN-BNL Fellow. The author would like to thank F. Zantow for correspondence and A. Patkós for careful reading of the manuscript and valuable suggestions.

References

1. T. Matsui, H. Satz, Phys. Lett. B **178**, 416 (1986)
2. T. Umeda, K. Nomura, H. Matsufuru, hep-lat/0211003
3. M. Asakawa, T. Hatsuda, Phys. Rev. Lett. **92**, 012001 (2004)
4. S. Datta, F. Karsch, P. Petreczky, I. Wetzorke, Phys. Rev. D **69**, 094507 (2004)
5. F. Karsch, Eur. Phys. J. C **43**, (2005)
6. T. Hatsuda, Eur. Phys. J. C **43**, (2005)
7. K. Petrov, Eur. Phys. J. C **43**, (2005)
8. L.D. McLerran, B. Svetitsky, Phys. Rev. D **24**, 450 (1981)
9. L.S. Brown, W.I. Weisberger, Phys. Rev. D **20**, 3239 (1979)
10. S. Nadkarni, Phys. Rev. D **33**, 3738 (1986)
11. O. Philipsen, Phys. Lett. B **535**, 138 (2002)
12. O. Kaczmarek, F. Karsch, P. Petreczky, F. Zantow, Phys. Lett. B **543**, 41 (2002)
13. S. Digal, S. Fortunato, P. Petreczky, Phys. Rev. D **68**, 034008 (2003)
14. O. Kaczmarek, F. Karsch, P. Petreczky, F. Zantow, Nucl. Phys. Proc. Suppl. **129**, 560 (2004)
15. O. Kaczmarek, F. Karsch, F. Zantow, P. Petreczky, Phys. Rev. D **70**, 074505 (2004)
16. P. Petreczky, K. Petrov, Phys. Rev. D **70**, 054503 (2004)
17. O. Kaczmarek, F. Zantow, work in progress; O. Kaczmarek, Eur. Phys. J. C **43**, (2005)
18. S. Digal, P. Petreczky, H. Satz, Phys. Lett. B **514**, 57 (2001)
19. G.S. Bali, Phys. Rept. **343**, 1 (2001)
20. N. Brambilla et al., hep-ph/0412158
21. C.J. Morningstar, K.J. Juge, J. Kuti, Nucl. Phys. Proc. Suppl. **73**, 590 (1999)
22. K.J. Juge, J. Kuti, C. Morningstar, Phys. Rev. Lett. **90**, 161601 (2003)
23. N. Brambilla, A. Pineda, J. Soto, A. Vairo, Nucl. Phys. B **566**, 275 (2000) [hep-ph/9907240]
24. O. Jahn, O. Philipsen, Phys. Rev. D **70**, 074504 (2004)
25. O. Kaczmarek, F. Karsch, P. Petreczky, F. Zantow, work in progress

26. S. Necco, R. Sommer, Phys. Lett. B **523**, 135 (2001); Y. Sumino, Phys. Rev. D **65**, 054003 (2002)
27. F. Zantow, Eur. Phys. J. C **43**, (2005)
28. F. Karsch, M.T. Mehr, H. Satz, Z. Phys. C **37**, 617 (1988)
29. G. Röpke, D. Blaschke, H. Schulz, Phys. Rev. D **38**, 3589 (1988)
30. T. Hashimoto et al., Z. Phys. C **38**, 251 (1988)
31. S. Digal, P. Petreczky, H. Satz, Phys. Rev. D **64**, 094015 (2001)
32. E.V. Shuryak, I. Zahed, Phys. Rev. D **70**, 054507 (2004); C.Y.L. Wong, hep-ph/0408020
33. E.V. Shuryak, Rev. Mod. Phys. **65**, 1 (1993)
34. Á. Mócsy, P. Petreczky, hep-ph/0411262
35. Yu.A. Simonov, hep-ph/0502078